Journal of the Geological Society of Sri Lanka
Vol. 14 (2011): 81-90.
C.B. Dissanayake Felicitation Volume

Electron microprobe dating of Monazites from Sri Lanka: implications on multiple thermal events related to Gondwana

Sanjeewa P.K. Malaviarachchi[*1] and Akira Takasu[2]

[1]Department of Geology, University of Peradeniya, Peradeniya, Sri Lanka.
[2]Department of Geoscience, Shimane University, Matsue 690-8504, Japan.
*(*Corresponding author, email: malavi@pdn.ac.lk)*

ABSTRACT

Monazites occur as inclusions in quartz, garnet, sillimanite and at quartz-plagioclase boundaries in a garnet granulite from the Highland Complex of Sri Lanka. These monazites appear as chemically distinct groups in the back scattered electron images and are classified as (i) unzoned, (ii) core-rim-type zoned and (iii) mesh-like zoned. Mesh-like zoned monazites document a new textural type not reported from elsewhere, and which probably originated during high temperature metamorphism of these rocks. Here we report electron microprobe U-Pb ages of separated monazites from the garnet granulite. Individual spot ages from electron microprobe analyses of the three distinct monazite categories are, 613-561 Ma (Group I), 728 - 619 Ma (Group II) and 516 - 460 Ma (Group III). The oldest monazite ages obtained in this study are in the range of ~ 700 to 728 Ma from the group (II) above, represent a new metamorphic age from Sri Lankan granulites which are believed to be of ~550-610 Ma metamorphic age according to published ages from the previous studies. The ages we obtained correspond to the thermal events associated with Kuunga and East African orogenies which occurred during the Gondwana amalgamation.

INTRODUCTION

Interpretation of the tectonics of the Earth has been much accurate and easy with the fast development of the geochronological instruments as well as improved analytical methods during the last decade. Dating of metamorphic and igneous events using accessory minerals such as zircon, monazite, xenotime, baddelyite etc. with high precision analytical techniques like SHRIMP, SIMS and electron microprobe has presently become very powerful owing to their improved capability to work under high spatial resolutions (Kelsey et al., 2003; Parrish, 1990). Using such analytical tools accompanied by X-ray elemental mapping, cathode-luminescence (CL) or back scattered electron (BSE) imaging techniques allows one to recognize chemical and chronological heterogeneities in accessory minerals, that was not possible during conventional geochronology. Thus, application of high resolution geochronology is recommended to avoid obtaining 'mixed ages' due to chemical heterogeneities in accessory minerals and it will enable one to understand true significance of analyses performed. Electron microprobe dating provides much higher spatial resolution than the ion microprobe and it too is a sample non-destructive method. Therefore, we used electron microprobe dating technique for Sri Lankan monazites in order to investigate its ability to unravel Gondwana tectonics.

Breakup of the Supercontinent Rodinia at ~750-800 Ma gave birth to the Gondwana Supercontinent by tectonic suturing of gigantic continental blocks of East and West Gondwana (Hoffman, 1999). West Gondwana comprised of African and South American continental blocks while the East Gondwana was formed of Madagascar, Australia, India, Antarctica and Sri Lanka. Dispersal of the Rodinia and the subsequent assembly of the Gondwana are considered as one of the most dynamic periods of the Earth's history. Thus, in order to understand this complex evolution of the Proterozoic to Lower Cambrian earth, careful dating is necessary.

Therefore, high resolution geochrono logical techniques play an important role to derive precise chronological information from rocks at multiple scales.

Assembly of the Gondwana super-continent has been one of the major topics of numerous geochronological studies over last two decades and has revealed several major tectonic events which apparently controlled the dynamics of the earth (e.g. Kröner, 2002). Meert (2003) suggested that the East Gondwana itself was not united, but its amalgamation occurred parallel to the assembly of final 'greater Gondwana' spanning from ~750-530 Ma. This is related to a series of orogenic processes involving continental fragments of East Africa, Arabian Nubian Shield, Seychelles, India, Madagascar, East Antarctica, Australia and Sri Lanka. Compiling >1000 U-Pb age data from the East Gondwana fragments, Meert (2003) classified them into two main tectonothermal events which are associated with the assembly of the East Gondwana. The first tectonic episode is the East African orogeny (Stern, 1994) at ~750-620 Ma forming the Mozambique belt as a result of the collision of India, Madagascar, Seychelles, East Antarctica and Sri Lanka against East Africa. The second is the Kuunga orogeny (Meert et al., 1995; Meert and Van Der Voo, 1997) which occurred during ~570-530 Ma as a consequence of the collision of Australia and East Antarctica against the continental blocks assembled at the East African orogene, and thus completing the amalgamation of the East Gondwana. Coeval to the Kuunga orogeny, the Brasiliano orogeny (Villenueve and Cornee, 1994) amalgamated the West Gondwana as a result of the collision of South America and Africa.

This study attempts to use electron microprobe-monazite dating techniques to the Sri Lankan basement rocks. Our data sheds light to understand the multiple thermal events associated with the Gondwana amalgamation, preserved in monazites. In addition, we newly report older metamorphic ages >700 Ma than the previously established 550–610 Ma (Kröner and Williams, 1993 and references therein) for the granulites of Sri Lanka.

The Sri Lankan Gondwana fragment

The Sri Lankan Precambrian consists of four distinct Proterozoic tectonic provinces (Fig. 1) namely; the Highland Complex, Wanni Complex, Vijayan Complex and Kadugannawa Complex (Kröner et al., 1991; Cooray, 1994). The Highland Complex is characterized by oldest crust formation ages of 2-3 Ga and granulite-facies metamorphism. The Wanni Complex and Kadugannawa Complexes are composed of upper-amphibolite- to granulite-facies rocks with 1-2 Ga crust formation age. The Vijayan Complex is an amphibolites-facies terrain of 1-2 Ga crust formation age (Kröner et al., 1987; Millisenda et al., 1988; Hölzl et al., 1994). Lithological details of each of these provinces are discussed in Kröner et al (2003) and previous geochronology is summarized by Kröner and Williams (1993).

Zircon geochronology has been applied to the Sri Lankan basement (e.g. Kröner et al., 1987; Baur et al., 1991; Kröner and Williams, 1993) to study protolith history and metamorphism of both ortho- and para-gneisses of the Highland Complex using sensitive high resolution ion microprobe (SHRIMP) and zircon-evaporation thermal ionization mass spectrometry (TIMS) techniques. These studies established the age of the granulite-facies metamorphism as 550-610 Ma. However, monazite dating of the Sri Lankan high grade rocks has been limited to only one conventional U-Pb analysis of monazite by Hölzl et al (1994).

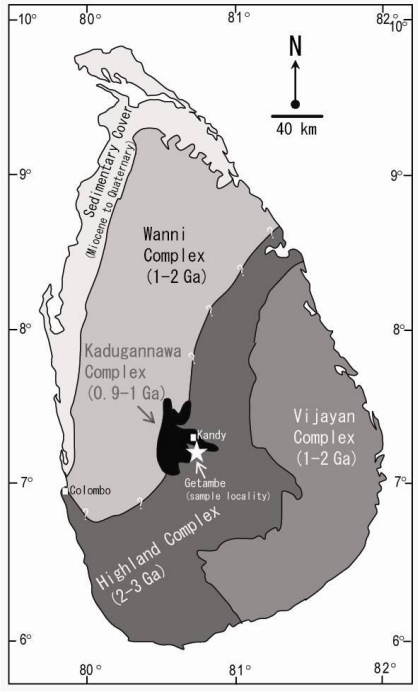

Figure 1: Simplified Geology map showing the subdivision of the Sri Lankan Precambrian (Cooray, 1994). Star indicates the location of the studied sample. The boundary between the Wanni Complex and the Highland Complex is not clearly defined so far (question marks).

Therefore, we investigated Sri Lankan monazites with the electron microprobe dating technique to understand their origin and evolution.

'CHIME' dating

The term CHIME abbreviates 'CHemical Isochron Method' (which was later renamed as 'chemical Th-U-total-Pb isochron method'), was first established by Suzuki and Adachi (1994, 1998) and Suzuki et al (1994), who dated zircon and monazite by electron microprobe. This dating method was further developed by Montel et al (1996). Subsequently, the CHIME method became enormously popular in many geochronological laboratories mainly because it is non-destructive, accurate, and fast, and has high spatial resolution.

Monazite is highly resistant to Pb loss during high temperature metamorphism (Copeland et al., 1988; Parrish, 1990; Suzuki et al., 1994). Monazite which is a Th and U rich can accumulate sufficient radiogenic Pb during ~100 Ma period to exceed detection limits of most electron microprobes (Suzuki and Adachi, 1998). Assuming that common Pb is negligible, and that partial loss or gain of Pb has not occurred (i.e. system remained closed), precise measurement of U, Th, and Pb by electron microprobe will give a geologically meaningful age even from a single monazite grain. If individual parts of a monazite grain and/or cogenetic monazite grains contain the same amounts of initial Pb but different Th and U, data will plot on a straight line (isochron), in the space of PbO (which includes both uranogenic and thorogenic Pb) against ThO_2 or UO_2. Using the slope of this best fit regression line and considering uncertainties in the microprobe analysis, an apparent age is calculated in the CHIME dating method (Suzuki and Adachi, 1998).

The CHIME dating technique has been developed primarily based on several assumptions (e.g. Kelsey et al., 2003). Main assumptions are, (1) all analyzed Pb is produced through radiogenic decay of Th and U in monazite, and (2) the analyzed monazite remained a closed system for Th, U and Pb following crystallization. The assumption of closed system behavior, however, cannot be directly tested where supporting geochronology (from other methods) is lacking (Kelsey et al., 2003). Importantly, studies have demonstrated (e.g. Williams et al., 1983; Corfu, 1988; Parrish, 1990) that the Pb inherited by monazite during its crystal growth or in other words common Pb, is generally low and therefore its effect on the calculated age is negligible. On the other hand, information on the closure temperature of monazite for Pb loss, and particularly its relevance for interpreting high temperature granulite-facies terrain is important and such knowledge is now expanding (e.g. Parrish, 1990). As a result, various studies have come out on estimates of closure temperature for Pb diffusion in monazite and most of them have proposed >900 ^{o}C (e.g. Copeland et al., 1988; Parrish, 1990; DeWolf et al., 1993; Suzuki et al., 1994; Dahl, 1997; Bingen and Van Breemen, 1998; Rubatto et al., 2001).

Sample selection and petrography

The studied monazite grains were separated from a garnet-biotite-sillimanite granulite (Sample 14A, Malaviarachchi and Takasu, 2005) from a quarry located at Getambe in the Highland Complex of Sri Lanka (Fig. 1). This garnet granulite exhibits well developed gneissic foliation. In some parts of the rock sillimanite-abundant layers are associated with boudins of mafic rocks which contain centimeter-scale snowball garnets.

The major mineral assemblage of the rock is garnet, biotite, quartz, sillimanite, plagioclase and K-feldspar. Spinel, zircon, monazite and opaque minerals occur as accessories. Garnet is the main porphyroblastic mineral, occurs in sizes of >5 mm, which is characterized by numerous inclusions of biotite, quartz, sillimanite, green-spinel and monazite. Except spinel and sillimanite, the other inclusion phases in garnet are not in direct contact with each other. Biotite and quartz inclusions are mainly found in the cores of garnet porphyroblasts, whereas sillimanite occurs in the mantle. Sillimanite also occurs as prismatic grains in the matrix, showing typical transverse fractures. Rims of some garnet porphyroblasts are replaced by sillimanite and/or biotite, or symplectite of biotite and quartz. In addition, fibrolite occurs associated with spinel. Biotite in the matrix forms a preferred orientation and is also found as random overgrowths on garnet rims. Plagioclase shows well developed polysynthetic twining and some contains exsolution lamella of K-feldspar forming antiperthite texture. Quartz commonly occurs in the matrix with plagioclase and K-feldspar. Ilmenite and rutile occur both as inclu-

sions in garnet as well as in the matrix with zircon.

This is the best sample showing multiple modes of occurrence of monazites in a single sample, among various granulites observed by the authors (Malaviarachchi, 2005; Malaviarachchi and Takasu, 2005). There are three modes of occurrence of monazite in the sample. Majority of the monazites occur as rounded to sub-rounded grains of ~0.15 mm within quartz or at quartz-plagioclase grain boundaries in the matrix (Fig. 2a). Some monazite grains occur in and around large sillimanite inclusions (~2.5 mm) of garnet porphyroblasts (Fig. 2b, c). These monazites are rounded to sub-rounded in shape, and usually <0.25 mm in size. In addition, there are elongated monazite inclusions (~0.15 mm) in garnet, mainly associated with spinel inclusions (Fig. 2d). Detailed petrography of the sample (Malaviarachchi, 2005; Malaviarachchi and Takasu, 2005) reveals that it is free from UHT minerals or assemblages like sapphirine, osumillite or spinel+quartz, and the highest metamorphic conditions are represented by sillimanite. Estimated pressure and temperature conditions of the sample are ~8 kbar and ~830 °C, respectively (Malaviarachchi, 2005).

SAMPLE PREPARATION AND ANALYSIS

The Sample 14A was crushed (~2.5 kg) using a jaw crusher and sieved to obtain a <250 µm whole rock fraction. Then, this fraction was washed with de-ionized water to remove light minerals (e.g. mica) and dried for 24 hours at 80 °C. After drying, highly-magnetic phases were removed using a bar magnet and then garnet and non-garnet fractions were obtained using a Frantz Isodynamic separator. The separated garnets were hand ground in a ceramic mortar to reduce the grain sizes further, in order to enable separation of monazite included in garnet. Subsequently, garnet-bearing (hand ground) and garnet-absent (after isodynamic separation) fractions were separately treated with heavy liquid (Di-iodomethane, density = 3.32 g/cm^3). The resulting heavy fractions were passed through Frantz Isodynamic separator order to separate monazite grains, and finally careful hand-picking under a binocular microscope was followed to choose monazite grains that are free of impurities. These selected monazites were mounted on glass slides and polished with 3 µm and then 1 µm diamond paste until the grains were thinned nearly to half of their original thickness. Then the grain mounts were carbon coated for subsequent analysis using JEOL JXA 8800M Electron Probe Micro Analyzer (EPMA) at Shimane University, Japan. Back Scattered Electron (BSE) images were used to investigate chemical zoning and to choose suitable grains and spots for analysis. Thirty representative grains were chosen from the separated monazite population (twenty from garnet-bearing fraction and ten from garnet-absent fraction) for dating.

Spot analyses were performed and dates were calculated for each spot using EPMA dating program for Microsoft-Excel® (Pommier et al., 2003). A total of 100 spots on the thirty monazite grains were analyzed for twelve elements (P, Si, Y, La, Ce, Pr, Nd, Sm, Gd, U, Th, Pb) using natural minerals and synthetic materials as calibration standards. Analytical conditions were maintained at 15 kV accelerating voltage, 80 nA probe current and 3 µm probe diameter. Th-M_α, U-M_β and Pb-M_α lines were used and the interferences of the Th with U-M_β and Y with Pb-M_α were corrected. Counting times of 50 s for Th and U, and 300 s for Pb were chosen for peak and background positions. After correction for background and interferences, the X-ray intensity data were converted into concentrations following the Bence and Albee (1968) method.

RESULTS AND DISCUSSION

The separated monazite grains were classified into three groups based on observations in BSE images. The Group 1 represents ~50-100 µm size sub-rounded to angular grains which appear unzoned in BSE images (Fig. 3a). The Group 2 consists of monazites of ~70-120 µm size range with angular edges, and zoned with a dark core and a bright rim part (Fig. 3b). Monazites of the Group 3 have an unusual zoning pattern (Fig. 3c). They are mostly elongated and ~100-200 µm in size showing nearly linear bright zones defining a 'mesh-like' zoning pattern in BSE images. Comparison of the BSE images of separated monazite grains with those of monazites in thin-sections reveal that the Groups 1, 2 and 3 correspond to the monazites in the matrix, monazites in the sillimanite porphyroblasts and monazites in garnet porphyro-

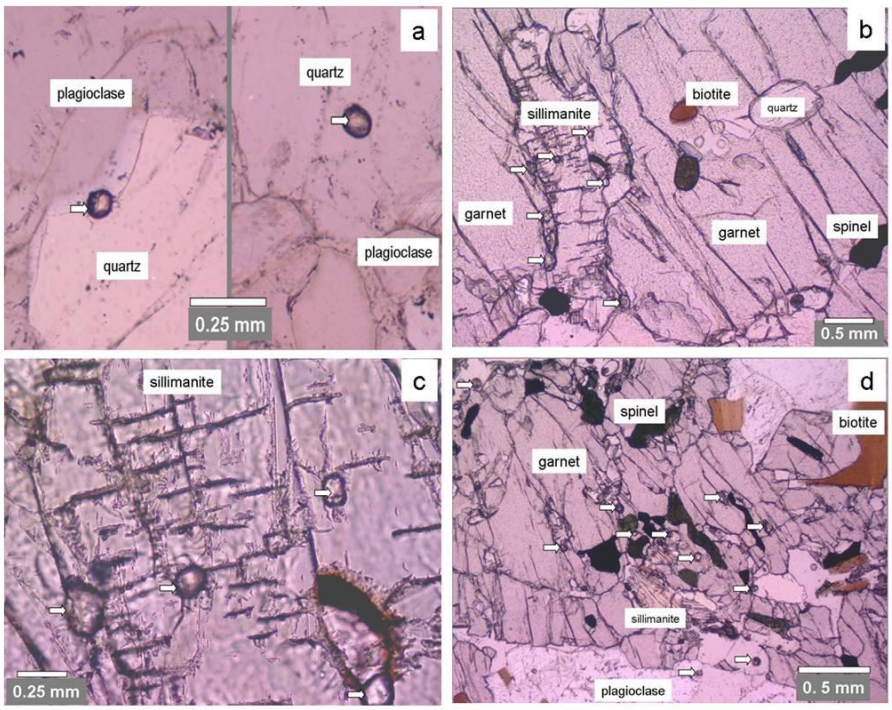

Figure 2: Photomicrographs showing different textural settings of monazite in the analyzed sample (plane polarized light). Monazite grains are marked with a white arrow for clarity. (a) Monazite grains in the matrix are commonly found as included in quartz or at quartz-plagioclase grain boundaries. (b) Tiny monazites are included in a porphyroblastic sillimanite found as an inclusion within a large garnet porphyroblast. Some monazites are aligned along the boundary of the sillimanite. Also, the garnet contains other inclusions of biotite, quartz and spinel. (c) An enlarged view of the sillimanite grain in (b), showing typical transverse fractures. (d) Numerous inclusions of monazites associated with spinel in a garnet porphyroblast.

-blasts, respectively (petrographic positions shown in the Fig. 2).

Table 1 gives ThO_2, UO_2 and PbO data of monazite from electron probe analysis and the calculated ages of the spots with 2σ uncertainty. On average, the Group 1 monazites have UO_2, ThO_2 and PbO contents of 0.260, 6.87 and 0.207 wt%, respectively. The Group 2 have greater average UO_2 and ThO_2 contents in their rims (UO_2= 0.254 and ThO_2= 6.94 wt %) than their dark cores (UO_2= 0.243 and ThO_2= 6.88 wt %). In contrast, PbO contents show an opposite relation with 0.241 and 0.226 wt% in the core and rim, respectively. Monazites of the Group 3 represent the lowest PbO contents among the three groups having relatively lower PbO content in the 'mesh part' (0.160 wt %) than in the areas away from the mesh (0.167 wt %). Contrary, UO_2 and ThO_2 contents are slightly higher in the mesh part (UO_2= 0.244 and ThO_2= 6.77 wt %) than those of the areas away from the mesh (UO_2= 0.242 and ThO_2= 6.04 wt %).

Fig. 3 summarizes the ranges of individual ages obtained from each point analysis marked on respective zones of the representative monazite grains. The Group 1 grains yield ages of 561 – 613 Ma (Fig. 3a). The Group 2 monazites have two age domains. Dark core regions represent ages of 673-728 Ma, while their bright rim parts have younger ages than the cores, in the range of 619-669 Ma (Fig. 3b). The youngest group is the Group 3 representing ages of 479-516 Ma where the bright 'linear areas' (mesh part) are relatively young with ages of 460-479 Ma than the areas away from the mesh part (dark areas) with age of 486-516 Ma (Fig. 3c). Average ages determined by tanh estimator (a technique used in CHIME dating; see Powell et al. 2002) are shown in the Table 2.

Calculation of 'isochron ages'

A plot of PbO against ThO_2* of the analyzed monazites are shown in the Fig. 4a. The ThO_2* represents the measured ThO_2 plus proportion of ThO_2 content converted from the measured UO_2 value (see Suzuki and Adachi, 1998 and Tickyj et al., 2004). Regression lines show that the three groups of monazites are clearly distinguishable from each other having different slopes for each group.

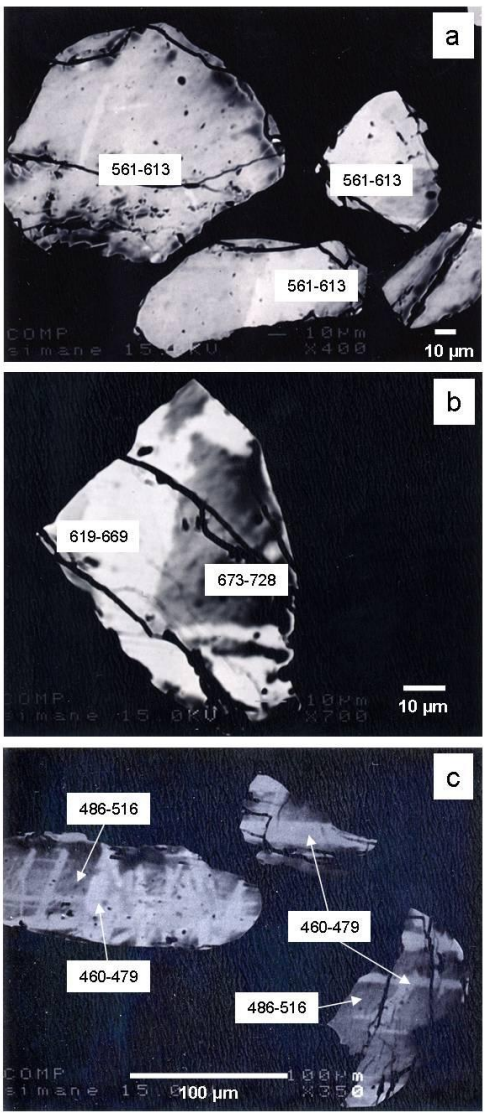

Figure 3: Back scattered electron images (BSE) of representative monazites with ages marked in million years (Ma). Bright zones in monazite represent relatively high Th-areas compared to dark zones. (a) Group 1 monazite grains (unzoned). (b) Group 2 monazites with dark cores and bright rim parts. (c) Group 3 monazites with an unusual zoning pattern ('mesh-like zoning'). Note nearly perpendicular cross cutting of linear Th-rich zones.

We observed a range of ages from 460 to 728 Ma from individual spots of the analyzed monazites (Table 1). For each group of monazites the 'isochron age' was calculated by the 'tanh estimator' using 'spot dates' and standard deviations of the each spot data. The methodology of the age calculation using 'tanh estimator' is found elsewhere (Powell et al., 2002; Kelsey et al. 2003).

The results are shown in the Table 2 and Fig. 4b. The mean isochron age of the Group 1 is 594±58 Ma. The cores of the Group 2 have a mean isochron age of 694±60 Ma and the rim portions have an age of 644±58 Ma. On the other hand, mesh parts of the Group 3 grains have mean isochron age of 473±56 Ma and the areas away from the mesh parts are of 497±57 Ma.

Implications of the monazite ages with respect to the Gondwana

Ages from the unzoned monazites (Group 1):

The age of the Group 1 grains, which are the most abundant of the analyzed monazite population (average age determined by tanh estimator of 594±58 Ma) is comparable to both East African and Kuunga orogenes. This age is consistent with the metamorphic ages of the Sri Lankan zircons (e.g. Kröner and Williams, 1993; Kröner et al., 2003). During these major tectonothermal events, we can expect a large growth/recrystallization of metamorphic monazites. We suggest that the Group 1 monazites formed in response to thermal events related to the waning stages of East African and/or Kuunga orogenies. Thus, it is clear that the Group 1 monazites are the most abundant in the sample and show no zonation, probably reflecting the origin at the time of high grade metamorphism of the sample. As a potential tectono-thermal event in Sri Lanka that could form the Group 1 monazites related to the Gondwana amalgamation, we suggest the collision of continental blocks of the Highland Complex vs. Wanni Complex, which were brought closer to each other by the East African orogeny (Kröner et al., 2003). This suggestion is consistent with the metamorphic ages of the Highland Complex granulites (550-610 Ma, Kröner et al., 2003) and the hypothesis of multiphase-amalgamation process by a series of 'local' events in many of the east Gondwana terrains, parallel to the assembly of the main Gondwana (Meert, 2003).

Ages from the core-rim zoned monazites (Group 2):

Age from the Group 2 grains is indicative of two-stage growth of the monazites. The cores of monazites in this group have older ages of 694±60 Ma and their corresponding rim portions have younger ages of 644±58 Ma (both representing average age determined by tanh estimator). This implies perhaps, that the older monazite grains (cores) may have been over-

Table 1: Analysis and geochronology results for the three groups of monazites (Oxide values in weight % from EPMA; age and age uncertainty 2σ in Ma).

	UO_2	ThO_2	PbO	Age	2σ (±)		UO_2	ThO_2	PbO	Age	2σ (±)
Group 1	0.188	6.84	0.205	611	60	Group 2 (rim)	0.207	6.58	0.204	625	61
	0.225	6.64	0.197	592	60		0.208	6.73	0.209	625	60
	0.323	7.01	0.221	608	55		0.256	6.71	0.213	625	59
	0.230	6.68	0.191	572	59		0.248	6.53	0.206	623	61
	0.193	6.99	0.210	611	59		0.270	6.87	0.217	622	58
	0.314	6.90	0.215	603	56		0.250	7.17	0.224	621	57
	0.185	6.71	0.192	584	60		0.266	7.28	0.236	642	56
	0.196	6.76	0.203	610	60		0.249	6.92	0.220	631	58
	0.378	7.05	0.226	604	54		0.248	6.90	0.221	636	59
	0.309	7.04	0.214	592	55		0.205	7.01	0.215	623	59
	0.325	7.07	0.225	613	55		0.316	7.06	0.235	643	56
	0.303	6.95	0.201	561	55		0.234	6.66	0.210	627	60
	0.215	6.61	0.185	561	59		0.197	6.88	0.214	632	60
Average	0.260	6.87	0.207				0.206	7.06	0.224	641	59
Group 2 (core)	0.195	6.72	0.229	690	62		0.265	7.40	0.235	630	55
	0.198	6.84	0.235	694	61		0.309	7.02	0.227	625	56
	0.197	6.88	0.238	699	61		0.320	7.01	0.230	634	56
	0.203	6.88	0.243	713	62		0.238	6.92	0.221	637	59
	0.219	6.81	0.248	728	62		0.307	7.06	0.231	636	56
	0.212	6.74	0.232	691	62		0.227	6.58	0.204	619	61
	0.219	6.67	0.237	709	62		0.172	6.60	0.206	638	62
	0.212	6.80	0.237	699	61		0.195	6.62	0.211	644	62
	0.198	6.90	0.234	687	61		0.237	6.63	0.218	653	61
	0.218	6.78	0.241	713	62		0.286	6.99	0.234	654	57
	0.234	6.85	0.247	717	61		0.290	7.00	0.235	654	57
	0.150	6.73	0.232	711	64		0.207	6.99	0.227	655	59
	0.278	6.87	0.241	687	59		0.273	6.65	0.225	660	60
	0.279	6.80	0.236	677	59		0.239	6.79	0.225	658	60
	0.277	6.91	0.240	679	59		0.254	6.85	0.227	656	59
	0.262	6.84	0.245	705	60		0.270	7.28	0.241	656	56
	0.305	7.03	0.254	701	58		0.283	7.49	0.251	660	55
	0.316	7.15	0.253	686	57		0.260	6.81	0.231	668	59
	0.215	7.02	0.242	695	60		0.253	6.86	0.232	668	59
	0.204	7.07	0.235	673	59		0.306	7.09	0.243	666	57
	0.297	7.09	0.251	688	57		0.324	7.47	0.256	665	54
	0.304	7.13	0.248	676	57		0.225	7.06	0.234	665	59
	0.325	7.09	0.252	683	57		0.205	7.05	0.232	666	59
	0.239	6.68	0.232	689	61		0.330	7.15	0.249	669	56
	0.230	6.61	0.229	689	62	Average	0.254	6.940	0.226		
	0.238	6.74	0.235	692	61	Group 3 (away	0.237	6.63	0.172	516	58
	0.249	6.70	0.235	692	61	from mesh)	0.229	6.67	0.163	491	57
	0.247	6.76	0.236	689	61		0.233	6.65	0.168	504	57
	0.294	6.94	0.247	692	58		0.255	6.74	0.169	497	56
	0.277	7.39	0.256	683	56		0.228	6.68	0.162	487	57
Average	0.243	6.880	0.241				0.239	6.69	0.167	497	57
('mesh part')	0.221	6.72	0.155	466	56		0.244	6.73	0.164	487	56
	0.243	6.81	0.156	460	55		0.272	6.78	0.173	502	56
	0.241	6.75	0.162	479	56		0.211	6.63	0.159	486	58
	0.246	6.76	0.162	479	56		0.278	6.80	0.174	503	55
	0.237	6.75	0.160	475	56		0.278	6.80	0.174	503	55
Average	0.244	6.772	0.160			Average	0.246	6.709	0.168		

grown by later metamorphic processes showing younger ages at the rim. Importantly, age of ~700 Ma (see Table 1) has not been reported in Sri Lanka so far as metamorphic age. Therefore, the Group 2 monazites document a new finding for the Sri Lankan granulites.

Ages from the mesh-like zoned monazites (Group 3):

Our finding of the Group 3 grains with an un-usual zoning pattern is significant, since to our knowledge there has been no earlier report on 'mesh-like' zoning patterns in monazite. This zoning pattern is clearly not an overgrowth

Table 2: U, Th and Pb oxide concentration ranges and calculated isochron ages for monazite grains (* uncertainty at 2σ level).

Monazite Group	wt% range			tanh derived
	UO_2	ThO_2	PbO	isochron age (Ma) *
Group 1	0.16 - 0.38	6.61 - 7.07	0.19 - 0.23	594 ± 38
Group 2 (core)	0.15 - 0.33	6.61 - 7.39	0.23 - 0.26	694 ± 26
Group 2 (rim)	0.17 - 0.33	6.53 - 7.45	0.21 - 0.26	644 ± 33
Group 3 ('mesh part')	0.22 - 0.27	6.72 - 6.85	0.16 - 0.17	473 ± 15
Group 3 (away from mesh)	0.21 - 0.28	6.63 - 6.80	0.16 - 0.17	497 ± 19

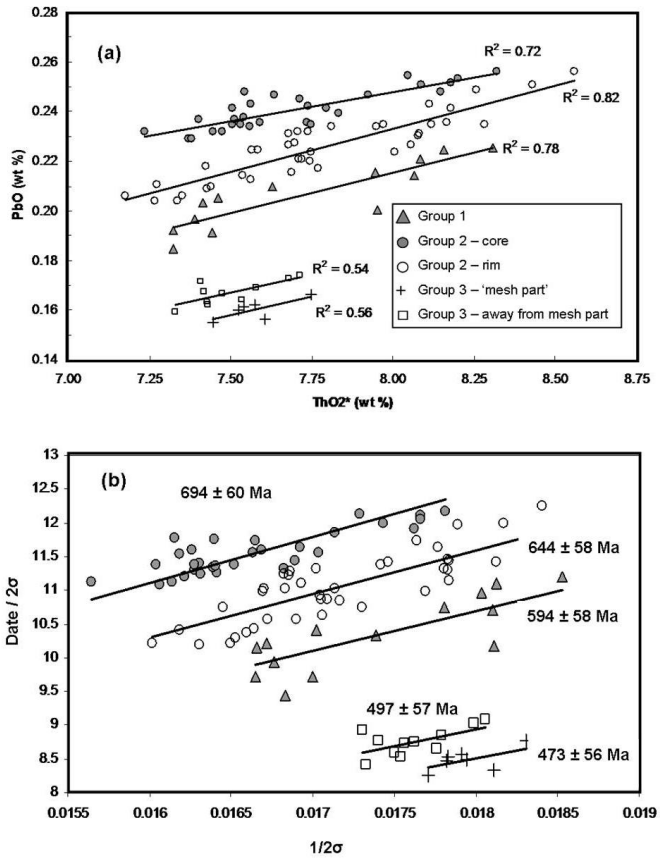

Figure 4: (a) A plot of PbO vs. ThO2* of analyzed grains showing linear correlations. Correlation coefficient (R^2) is also shown. (b) A plot of the ratio of date: 2σ uncertainty of each spot vs. the reciprocal of 2σ uncertainty. Isochron ages of each monazite group were calculated using the tanh estimator (see text).

since the zoned region is located within the crystal. On the other hand, such zoning pattern may occur due to late stage fluid migration along fractures or cleavages within the crystal. Also, it is evident from the BSE images of these grains that the zoning is more-or-less linear which intersect each other approximately at right angles. If these zones of relatively high Th compared to dark areas of the same grain reflect traces of fluid migration and subsequent Th enrichment through fractures, then the mechanism of formation of such a systematic fracture pattern may be important, due to the fact that it is unlikely for monazite crystal to have nearly perpendicular perfect cleavages. Therefore, more detailed investigation is necessary to explain the mechanism of the formation of this mesh like zoning patterns in monazite. However, we do not attempt to explain the mechanism at this stage since it is beyond the scope of this paper.

Ages of mesh like zoned monazites are relatively young (460-516 Ma; average age determined by tanh estimator) compared to the estimated age of the Gondwana amalgamation period (530-750 Ma; Meert, 2003). Therefore,

we suggest that the Group 3 monazites document relic, but probably a less-common evidence of a thermal event at the extreme late parts of the Gondwana assembly process. However, if one considers the above suggestion that bright zones of the mesh like monazites may reflect Th enrichment by fluid migration, then the ages of bright zones would definitely reflect a cooling event. Therefore, at least the age obtained from the areas away from the bright regions (497±57 Ma; average age determined by tanh estimator) would record the formation ages of these grains, and might be related to the tectonics of the latter periods of the Kuunga orogeny.

Thus, the above results reflect the fact that the EPMA dates obtained in this study are in reasonable agreement with those obtained by zircon data. In addition, it is clear that monazites could be preserving a history that is not currently known fully from zircons since their textural significance have not been given adequate consideration.

CONCLUSIONS

The analyzed sample depicts a fair distribution of monazites which are possibly formed under three different petrographical settings. Mesh-like zoned monazite document new textural evidence preserved in the grains which has not been reported elsewhere, and it possibly formed during high temperature metamorphism of these rocks. The monazite ages from individual spot analysis record multiple tectonic history related to the East African and Kuunga orogenes of the Gondwana from ~728 to ~460 Ma (i.e. the time span derived from the three groups of monazites here). Therefore, we conclude that the age range of high-grade granulite-facies metamorphism of the Sri Lankan basement could be broader than the current understanding of ~550-610 Ma reported from zircons by previous studies. Importantly, this set of data highlights the necessity to do more texture-based zircon/monazite analysis.

Acknowledgements

Our thanks to B. Roser, M. Akasaka, H. Komuro, H. Ohira, A. Kamei and the members of the Metamorphism Seminar (2003-2004) of the Shimane University, Japan for fruitful discussions. T. Sakurai is thanked for technical assistance and B. Reno for suggestions and helps on age calculations with the software. Comments and suggestions by Philippe Goncalves, A. Kröner, R. Parrish and L.R.K. Perera on a previous version significantly improved the manuscript.

REFERENCES

Baur, N., Kröner, A., Liew, T.C., Todt, W., Williams, I.S. and Hofmann, A.W. (1991) U-Pb isotopic systematics of zircons from prograde and retrograde transition zones in high-grade orthogneisses, Sri Lanka. J. Geol., 99: 527-545.

Bence A.E. and Albee, A.L. (1968) Empirical correction factors for the electron microanalysis of silicates and oxides. J. Geol., 76: 382-403.

Bingen, B. and VanBreemen, O. (1998) U-Pb monazite ages in amphibolite- to granulite-facies orthogneiss reflect hydrous mineral breakdown reactions: Sveconorwegian Province of SW Norway. Contrib. Mineral. Petrol., 132: 336–353.

Cooray, P. G. (1994) The Precambrian of Sri Lanka - a historical review. Precamb. Res., 66: 3-20.

Copeland, P., Parrish, R.R. and Harrison, T.M. (1988) Identification of inherited radiogenic Pb in monazite and its implications for U-Pb systematics. Nature, 333: 760–763.

Corfu, F. (1988) Differential response of U-Pb systems in coexisting accessory minerals, Winnipeg River Sub-province, Canadian Shield: implications for Archean crustal growth and stabilization. Contrib. Mineral. Petrol., 98: 312–325.

Dahl, P.S. (1997) A crystal-chemical basis for Pb retention and fission track annealing systematics in U-bearing minerals, with implications for geochronology. Earth Planet. Sci. Lett., 150: 277–290.

DeWolf, C.P., Belshaw, N. and O'Nions, R.K. (1993) A metamorphic history from micron-scale 207Pb/206Pb chronometry of Archean monazite. Earth Planet. Sci. Lett., 120: 207–220.

Hoffman, P.F. (1999) The break-up of Rodinia, birth of Gondwana, true polar wander and Snowball Earth. J. Afri. Earth Sci., 28: 17-33.

Hölzl, S., Hofmann, A.W., Todt, W. and Kohler, H. (1994) U-Pb geochronology of the Sri Lankan basement. Precamb. Res., 66: 123-149.

Kelsey, D.E., Powel, R., Wilson, C.J.L. and Steel, D.A. (2003) (Th+U)-Pb monazite ages from Al-Mg-rich metapelites, Rauer Group, east An-

tarctica. Contrib. Mineral. Petrol., 146: 326-340.

Kröner, A. (2002) The Mozambic Belt of East Africa and Madagascar: significance of zircon and Nd model ages for Rodinia and Gondwana supercontinent formation and dispersal. South African J. Geol., 105: 151-167.

Kröner, A., Cooray, P.G. and Vitanage, P.W. (1991) Lithotectonic subdivision of the Precambrian basement in Sri Lanka. Geol. Surv. of Sri Lanka, Professional Paper 5; 5-21.

Kröner, A., Kehelpannala, K.V.W. and Hegner, E. (2003) Ca. 750-1100 Ma magmatic events and Grenville-age deformation in Sri Lanka: relevance for Rodinia supercontinent formation and dispersal, and Gondwana amalgamation. J. Asian Earth Sci., 22: 279-300.

Kröner, A. and Williams, I.S. (1993) Age of metamorphism in the high-grade rocks of Sri Lanka. J. of Geol., 101: 513-521.

Kröner, A., Williams, I.S., Compston, W., Baur, N., Vitanage, P.W. and Perera, L.R.K. (1987) Zircon ion microprobe dating of Precambrian high-grade rocks in Sri Lanka. J. Geol., 95: 775-791.

Malaviarachchi, S. (2005) Petrological study of High-grade metamorphic rocks from Central Sri Lanka. M.Sc Thesis, Graduate School of Science and Engineeering, Shimane University, Japan.

Malaviarachchi, S. and Takasu, A. (2005) Petrographic study on the high-grade metamorphic rocks from the Highland and Kadugannawa Complexes, central Sri Lanka. Geoscience Reports, Shimane University 24: 31-46.

Meert, J.G. (2003) A synopsis of events related to the assembly of eastern Gondwana. Tectonophysics, 362; 1-40.

Meert, J.G. and Van der Voo, R. (1997) The assembly of Gondwana 800-550 Ma. J. of Geodynamics, 23: 223-235.

Meert, J.G., Van der Voo, R. and Ayub, S. (1995) Paleomagnetic investigation of the late Proterozoic Gagwe lavas and Mbozi complex, Tanzania and the assembly of Gondwana. Precamb. Res., 74: 225-244.

Milisenda, C.C., Liew, T.C., Hofmann, A.W. and Kröner, A. (1988) Isotopic mapping of age provinces in Precambrian high-grade terrains: Sri Lanka. J. Geol., 96: 608-615.

Montel, J-M., Foret, S., Veschambre, M., Nicollet, C. and Provost, A. (1996) Electron microprobe dating of monazite. Chem. Geol., 131: 37–53.

Parrish, R.R. (1990) U–Pb dating of monazite and its application to geological problems. Canadian J. Earth Sci., 27, 1431– 1450.

Pommier, A., Kocherie, A. and Legendre, O. (2003) EPMA dating: a program for age calculation from electron microprobe measurements of U-Th-Pb. Geophysical Research Abstracts 5, 09054, European Geophy. Society.

Powell, R., Hergt, J. and Woodhead, J. (2002) Improving isochron calculations with robust statistics and the bootstrap. Chem. Geol., 185: 191-204.

Rubatto, D., Williams, I.S. and Buick, I.S. (2001) Zircon and monazite response to prograde metamorphism in the Reynolds Range, central Australia. Contrib. Mineral. Petrol., 140: 458–468.

Stern, R.J. (1994) Arc assembly and continental collision in the Neoproterozoic East African Orogen: implications for the consolidation of Gondwanaland. Annual Rev. of Earth and Planet. Sci., 22: 319-351.

Suzuki, K. and Adachi, M. (1994) Middle Precambrian detrital monazite and zircon from the Hida gneiss on Oki-Dogo island, Japan: their origin and implications for the correlation of basement gneiss of Southwest Japan and Korea. Tectonophysics 235: 277-292.

Suzuki, K. and Adachi, M. (1998) Denudation history of the high T/P Ryoke metamorphic belt, southwest Japan: constraints from CHIME monazite ages of gneisses and granitoids. J. Metamorphic Geol., 16: 23-37.

Suzuki, K., Adachi, M. and Kajizuka, I. (1994) Electron microprobe observations of Pb diffusion in metamorphosed detrital monazites. Earth and Planet. Sci. Lett., 128: 391-405.

Tickyj, H., Hartmann, L.A., Vasconcellos, M.A.Z., Philipp, R.P. and Remus, M.V.D. (2004) Electron microprobe dating of monazite substantiates ages of major geological events in the southern Brazilian shield. J. South American Earth. Sci., 16: 699-713.

Villenueve, M. and Cornee, J. (1994) Structure, evolution and paleogeography of the West African craton and bordering belts during the Neoproterozoic. Precamb. Res., 69: 307-327.

Williams, I.S., Compston, W. and Chappell, B.W. (1983) Zircon and monazite U-Pb systems and the histories of I-type magmas, Berridale Batholith, Australia. J. Petrol., 24: 76–97.